Article

Shake-Off Process in Non-Sequential Single-Photon Double Ionization of Closed-Shell Atomic Targets

Anatoli S. Kheifets (ID)

Research School of Physics, The Australian National University, Canberra, ACT 2601, Australia;
a.kheifets@anu.edu.au

Abstract: Amusia and Kheifets in 1984 introduced a Green's function formalism to describe the effect of many-electron correlation on the ionization spectra of atoms. Here, we exploit this formalism to model the shake-off (SO) process, leading to the non-sequential single-photon two-electron ionization (double photoionization—DPI) of closed-shell atomic targets. We separate the SO process from another knock-out (KO) mechanism of DPI and show the SO prevalence away from the DPI threshold. We use this kinematic regime to validate our model by making a comparison with more elaborate techniques, such as convergent and time-dependent close coupling. We also use our model to evaluate the attosecond time delay associated with the SO process. Typically, the SO is very fast, taking only a few attoseconds to complete. However, it can take much longer in the DPI of strongly correlated systems, such as the H^- ion as well as the subvalent shells of the Ar and Xe atoms and Cl^- ion.

Keywords: atomic photoionization; many-electron correlation; non-sequential double ionization

PACS: 32.80.Rm 32.80.Fb 42.50.Hz

1. Introduction

The simultaneous removal of two electrons from an atom following absorption of a single photon is an archetypal process driven entirely by many-electron correlation. Such a non-sequential single-photon two-electron ionization (double photoionization or DPI in short) has been the focus of experimental and theoretical activities for several decades [1–3]. The correlation mechanisms of DPI are well understood and can be described as the shake-off (SO) and knock-out (KO) processes [4–7]. Shake-off is driven by a sudden change of the atomic potential after a fast removal of the primary photoelectron. Conversely, knock-out is a slow process in which the departing electron impinges on the ionic core and ejects the secondary photoelectron. A complementary quasi-free mechanism (QFM) of PDI, in which the nucleus remains a spectator, was predicted theoretically by Amusia and co-workers [8]. Recently, the QFM was studied experimentally [9–11], and it was ascribed to a combination of the SO and KO processes.

The first theoretical description of DPI in atoms invoked the lowest order perturbation theory [12–15]. With a growing computational power, more sophisticated non-perturbative methods were developed. The convergent close-coupling (CCC) [16,17] and the time-dependent close-coupling (TDCC) [18] are among the many predictive and accurate numerical techniques.

A resurged interest in DPI was stimulated by a newly acquired experimental capability to resolve atomic photoionization in time. Laser pulses are shaped in such a way that they can probe atomic ionization on the attosecond (1 as = 10^{-18} s) time scale. Firstly, single photoionization was time resolved [19,20]. Then a DPI process was traced in time [21]. The accompanying theoretical studies have also appeared [22,23].

An alternative theoretical approach to DPI can be provided by the single-hole Green's function (SHGF) formalism introduced to photoionization [24,25]. Originally, this method

was utilized to calculate shake-up satellites in atomic photoionization spectra [26–29]. However, by construction, the SHGF contains the DPI continuum, which can be attributed to the SO process. This capability of the SHGF method has been overlooked so far. Here, we rectify this omission.

The present work is structured in the following way. We start with a brief introduction of the SHGF technique, using a diagrammatic expansion of the ionization amplitude. We identify the double ionized continuum in this amplitude and link it with the imaginary part of the SHGF self-energy. This allows us to derive the analytic expressions for the DPI cross section resolved with the photoelectron energy as well as the time delay associated with the SO process. Next, we test our energy resolved DPI cross sections against experiments as well as the earlier CCC and TDCC calculations. This way, we identify the photoelectron energy range where the SO process makes the dominant contribution to DPI. Finally, we evaluate the time that it takes to shake off a bound electron. As expected, the SO process is fast with only a few attoseconds needed to shake off the secondary photoelectron into the two-electron continuum. However, there are few notable exceptions when the SO process takes much longer time to complete. We find this situation in strongly correlated targets such as the negative H^- ion as well as the subvalent shells of the Ar and Xe atoms and the Cl^- ion. The binding of the H^- ion is wholly owed to many-electron correlation, and the photoionization of subvalent ns shells in Ar, Xe and Cl^- is affected very strongly by correlation satellites. As the result, the SO process in H^- takes as much as 30 as, whereas the similar process in Ar $3s$ and Xe $5s$ requires nearly 50 as to complete. The same process in Cl^- $3s$ takes in excess of 100 as. We conclude by evaluating other components of the measurable time delay in DPI and thus making the case for the experimental resolution of the SO process in time.

2. Theory

The SO process leading to the ejection of two electrons in the continuum can be exhibited graphically by an infinite sequence of diagrams presented in Figure 1a. Here, we use the following graphical symbols. A straight line with an arrow to the right represents the electron continuum states k, f whereas an arrow pointing to the left exhibits the holes in atomic shells i, l, m. Before photoabsorption, all the atomic shells are presumed to be fully occupied and thus closed. The atomic ground state (the "vacuum" state) contains neither holes nor excited electrons. The wavy line denotes the Coulomb interaction between the electrons. The dashed line represents an absorbed photon. A circle denotes the diagonal matrix element of the self-energy part of the Green's function Σ_i. The SHGF self-energy is expanded graphically in more detail in Figure 1b.
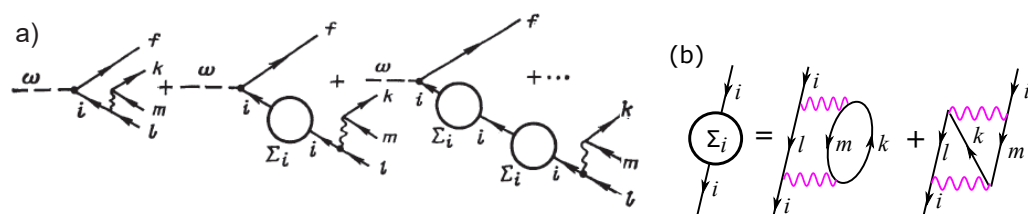

Figure 1. (**a**) Schematic representation of the SO process leading to a two-electron continuum. The circle represents the self-energy part of the SHGF expanded in more detail in (**b**).

The corresponding DPI amplitude can be found by summing a geometric progression of terms in Figure 1a that leads to the following expression:

$$\langle f\|M_{SO}\|i\rangle = \langle f\|r\|i\rangle \left(1 - \frac{\Sigma_i(\varepsilon)}{\varepsilon - \epsilon_i - i\delta}\right)^{-1} \frac{\langle ik\|U_L\|lm\rangle}{\varepsilon - \epsilon_i - i\delta} . \tag{1}$$

Here, $\langle f\|r\|i\rangle$ is a dipole matrix element of the single-photon absorption and $\langle ik\|U_L\|lm\rangle$ is a Coulomb matrix element, which includes a direct and exchange $l \leftrightarrow m$ terms and

involves a transfer of the angular momentum L. Both the dipole and Coulomb matrix elements are reduced to strip their angular momentum projections dependence. The symbol $\varepsilon = \epsilon_f - \omega < 0$ denotes an effective hole energy. In the absence of correlation, $\varepsilon = \epsilon_i$ is the orbital energy. Many-electron correlation adds a discrete spectrum of shake-up satellites and a shake-off continuum, which starts at the DPI threshold $E_\infty = \epsilon_l + \epsilon_m$. The infinitesimally small $\delta \to 0$ in the energy denominator defines the pole bypass.

The imaginary part of Equation (1) gives rise to an additional phase of the DPI amplitude due to the final state correlation:

$$\arg M_{\text{SO}} = \arctan \frac{\text{Im}\Sigma_i(\varepsilon)}{\text{Re}[\varepsilon - \epsilon_i - \Sigma_i(\varepsilon)]} \approx \arctan \frac{\text{Im}\Sigma_i(\varepsilon)}{\text{Re}[\varepsilon - \epsilon_i]} . \tag{2}$$

Here $\text{Im}\Sigma_i = \pi (2L+1)^{-1} |\langle ik \| U_L \| lm \rangle|^2$. The approximate equality is satisfied under the condition that $|\varepsilon - \epsilon_i| \gg |\Sigma_i(\varepsilon)|$. This condition defines the part of the double ionized continuum sufficiently far from the main photoelectron line.

The energy resolved single-differential cross-section (SDCS) is given by Equation (9) of [25]:

$$\frac{d\sigma_i^{2+}}{d\epsilon_f} = \sigma_i^+ \frac{1}{\pi} \frac{\text{Im}\Sigma_i(\varepsilon)}{|\varepsilon - \epsilon_i - \Sigma_i(\varepsilon)|^2} \approx \sigma_i^+ \frac{1}{\pi} \frac{\text{Im}\Sigma_i(\varepsilon)}{|\varepsilon - \epsilon_i|^2} . \tag{3}$$

By solving this equation relative to $\text{Im}\Sigma_i$, we can express the additional phase of the DPI amplitude due to the final state correlation in the following form:

$$\arg M_{\text{SO}} = \arctan \frac{\pi}{\sigma_i^+} \frac{d\sigma_i^{2+}}{d\epsilon_f} |\varepsilon - \epsilon_i| . \tag{4}$$

We note that all the quantities entering this expression are known from the experiment, which are the single photoionization cross-section of the primary photoelectron σ_i^+ and the energy differential DPI cross-section $d\sigma_i^{2+}/d\epsilon_f$.

By integrating the SDCS Equation (3) over the fast photoelectron energy, we can obtain the double-to-single photoionization cross-section ratio:

$$R = \frac{\sigma^{2+}}{\sigma^+} = \frac{1}{\sigma^+} \int_0^\infty \frac{d\sigma^{2+}}{d\epsilon_f} d\epsilon_f . \tag{5}$$

This ratio is known in He, and its isoelectronic sequence of ions [30]. It will serve as a convenient reference in Section 3.2.

Following [25], we can introduce the inverse SHGF

$$F(\varepsilon) = G^{-1}(\varepsilon) = \varepsilon - \epsilon_i - \Sigma_i(\varepsilon) \tag{6}$$

Then the argument of the SO amplitude Equation (2) can be rewritten as

$$\arg M_{\text{SO}} = \arg G^{-1}(\varepsilon) = \arg F(\varepsilon) \tag{7}$$

This expression allows to use the integral rule presented by Equation (5) of [25], which relates the energies of the discrete shake-up satellites with the time delay:

$$\sum_{k=0}^\infty (\varepsilon_k - E_k) = \frac{1}{\pi} \int_{-\infty}^{E_\infty} \varepsilon \tau(\varepsilon) \, d\varepsilon , \text{ where } \tau(\varepsilon) = \frac{\partial}{\partial \varepsilon} \arg M_{\text{SO}} = \frac{\partial}{\partial \varepsilon} \arg F(\varepsilon) \tag{8}$$

Here $E_k = \epsilon_l + \epsilon_m - \epsilon_k$ and $E_0 = \epsilon_i$ are non-correlated energies of the shake-up excitations calculated from the HF orbital energies. Meanwhile, ε_k are the corresponding energies shifted by the final-state correlation and found as the poles of the SHGF. The integral time

delay rule Equation (8) presents an analytical test for the numerical SO time delay values. This test will be conducted in Section 3.3.

3. Numerical Results

3.1. Computation Details

We use the ATOM suite of programs developed by Miron Amusia and co-workers [31]. The SCFHF and FCHF computer codes calculate the atomic ground and excited states in the self-consistent and frozen-core Hartree–Fock (HF) approximations, respectively. Then the Coulomb matrix elements are evaluated, and the SHGF and its self-energy are found. The latter are used to calculate the SDCS, the R ratio and the time delay associated with the SO process.

We consider the two types of the SO process. In the first type, all the hole states i, l, m are confined to the same ns shell. The fast primary photoelectron is ejected from this shell into the p-continuum, whereas the slow electron is shaken off into the s-continuum. Such an intra-shell SO process takes place in the outer valence shell of the He, Be and Mg atoms as well as the H^- ion. The second inter-shell type of the SO process accompanies ionization of the sub-valent ns shells of noble gas atoms Ne, Ar and Xe. While the primary hole i is made in the ns shell, the secondary holes l, m are made in the outermost np shell. The primary fast photoelectron is ejected in the p-wave, whereas the secondary electron is shaken off primarily into the d-wave.

3.2. Energy Resolved DPI Cross-Sections

In Figure 2, we exhibit the energy resolved DPI cross section of helium at the excess energies above the DPI threshold $E = 100, 450$ and 720 eV (from left to right). The SDCS Equation (3) is symmetrized by adding the two energy distributions of the slow and fast photoelectrons, thus giving it a characteristic U-shape. The present shake-off calculations using Equation (3) are compared with various reference data indicated in the figure caption. The integrated cross-sections of single photoionization σ_{1s}^+ are used as tabulated in [32]. We can observe in Figure 2 that the SO mechanism is becoming gradually dominant as the photon energy grows. This is particularly true for a highly asymmetric energy sharing between the photoelectrons. Under this kinematics, the primary photoelectron takes nearly all the photon energy and is ejected in the dipole channel as a p-wave. At the same time, the secondary SO photoelectron is very slow and is ejected almost isotropically as an s-wave in the intra-shell SO process. It is this characteristic photoelectron angular distribution that was observed experimentally in He at $E = 450$ eV [7].
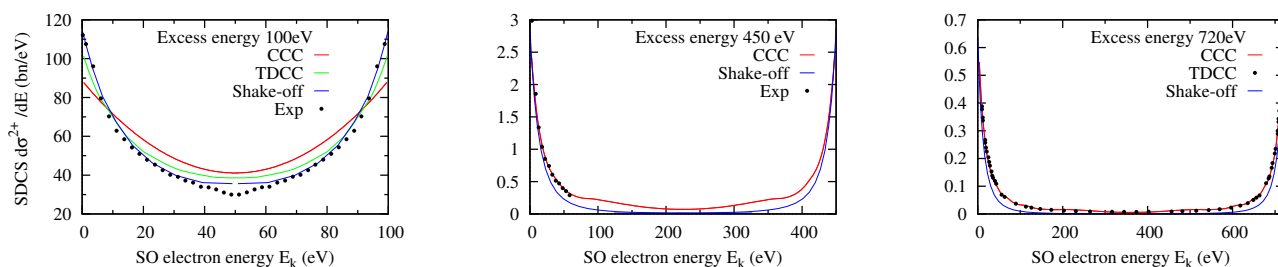

Figure 2. The energy resolved DPI cross-section of helium $d\sigma^{2+}/dE)$ (in bn/eV) at the excess energies above the DPI threshold $E = 100, 450$ and 720 eV (from left to right). The present shake-off calculations using Equation (3) are compared with the following reference data. At $E = 100$ eV, the relative measurement [33] is normalized to the TDCC calculation [34] and shown along with an analogous CCC calculation [35]. At $E = 450$ eV, the relative experiment [7] is normalized to the CCC calculation from the same reference. At $E = 720$ eV, the TDCC [36] and the CCC [11] calculations are shown.

Meanwhile, the equal energy sharing between the photoelectrons is affected by a competing KO process and deviates from the present SO predictions. This deviation, which is strongest at $E = 100$ eV, can also be seen at higher photon energies near the mid-point of the photoelectron energy distribution.

The double-to-single ratios as calculated by the SO model using Equation (5) are presented in Table 1. The SO ratio in He is equal to 1.44%, which is very close to the CCC ratio of 1.67% [30]. For other targets, this comparison is less accurate, especially for the H$^-$ ion, which is twice overestimated, while Be and Mg are 50% underestimated.

Table 1. Asymtptoc double-to-single cross-section ratios in various targets as calculated by the SO model using Equation (5) and compared with earlier CCC calculations.

Target	E_0	Threshold	Raio, %		Ref.
	Ry	**Ry**	**SO**	**CCC**	
He 1s	1.836	5.807	1.44	1.67	[30]
H$^-$ 1s	1.000	1.055	3.43	1.60	[30]
Be 2s	0.618	1.951	0.26	0.37	[37]
Mg 3s	0.506	1.558	0.16	0.25	[38]

3.3. Time Delay

Results of the time delay calculations by taking the energy derivative of the SO phase Equation (2) are displayed in Figure 3. The horizontal axis in the figure denotes the slow photoelectron energy. It is assumed that the photon energy is very large and nearly all of it is carried away by the second fast photoelectron. The three panels of this figure display the time delay results for the He 1s, Be 2s, Ne 2s and Mg 3s (left), H$^-$ 1s (center) and Ar 3s, Cl$^-$ 3s and Xe 5s (right). We observe a very small SO time delay in He 1s not exceeding a few attoseconds. A similarly small time delay is found in the intra-shell SO process in Be 2s and Mg 3s as well as the inter-shell SO process in Ne 2s. Incidentally, the time delay in the inner 1s shell of Be is much smaller than that in the valence 2s shell, the reason being the Coulomb field of the bare nucleus, which makes many-electron correlation and associated time delay negligible.

The SO time delay in H$^-$ 1s is markedly higher by nearly an order of magnitude. Time delay grows further in Ar 3s and Xe 5s, while it exceeds the 100 as mark in the negative Cl$^-$ ion. We relate this growth of time delay to much bolder shake-up and shake-off processes in these targets, which are strongly affected by many-electron correlation.

Another indication of this effect is presented in Table 2. Here we compare the summary displacement of the main and shake-up satellite lines in the photoelectron spectra of He 1s and Ar 3s with the corresponding time delay integral Equation (8). We observe in this table that the many-electron correlation causes a much stronger line displacement in Ar than in He. This is matched by a much larger SO time delay in Ar in comparison with He.
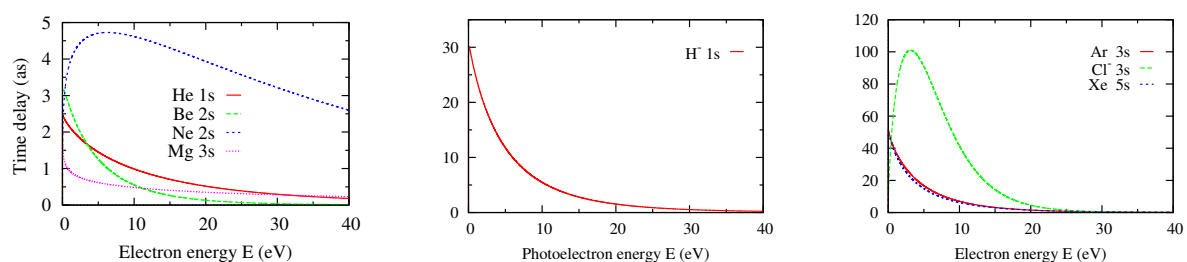

Figure 3. Shake-off time delay (in attoseconds) in He 1s, Be 2s, Ne 2s and Mg 3s (**left**), hydrogen H$^-$ 1s (**center**) and Ar 3s, Cl$^-$ 3s and Xe 5s (**right**), calculated by taking the energy derivative of the SO phase Equation (2).

Table 2. The energies of the shake-up satellites in the photoelectron spectra of He $1s$ and Ar $3s$ as calculated in the HF approximation E_k and as the poles of the SHGF ε_k. The sum $\sum_k (E_k - \varepsilon_k)$ in each target is compared with the corresponding time delay integral Equation (8).

k	E_k	ε_k	$E_k - \varepsilon_k$
	Helium $1s$		
0	1.8360	1.7287	0.1073
1	4.7360	4.8053	−0.0693
2	5.3540	5.3622	−0.0082
3	5.5540	5.5568	−0.0028
4	5.6460	5.6473	−0.0013
5	5.6950	5.6957	−0.0007
Sum			0.0250
SO integral Equation (8)			0.025
k	E_k	ε_k	$E_k - \varepsilon_k$
	Argon $3s$		
0	2.5550	2.1508	0.4042
1	2.5920	2.8389	−0.2469
2	2.9630	3.0235	−0.0605
3	3.1070	3.1274	−0.0204
4	3.1780	3.1879	−0.0099
5	3.2180	3.2235	−0.0055
Sum			0.0610
SO integral Equation (8)			0.063

4. Summary and Outlook

In the present work, we demonstrated that the SO process is prevalent in DPI at large photon energies exceeding significantly the double ionization threshold. Under this condition, the two-electron energy sharing is highly asymmetric with the primary photoelectron taking nearly all of the photon energy, while the secondary SO electron is rather slow. The slow electron can be delayed by repeated interaction with the ionic core. In the intra-shell shake-off process, this interaction is confined to the same shell and is typically rather quick. The intra-shell SO processes in He $1s$, Be $2s$ and Mg $3s$ take no more than several attoseconds to complete. The marked exception is the intra-shell SO in the H$^-$ ion, which may take several tens of attoseconds. We attribute this effect to a strongly correlated nature of H$^-$ which will not bind in the absences of correlation. The inter-shell SO process are more involved and take typically longer time. We observe a considerable delay in the SO of Ar $3s$ and Xe $5s$. The Cl$^-$ ion, which is iso-electronic to Ar, demonstrates a very significant SO delay exceeding 100 as. All these targets are prone to strong final-state correlation and display intense shake-up satellite spectra with a strong line displacement relative to the corresponding HF energies. The only exception is the inter-shell SO in Ne, which is still rather quick.

It is instructive to compare the SO time delay in DPI with the analogous characteristic of single photon one-electron ionization (single photoionization—SPI). The energy derivative of the SPI amplitude is known as the Wigner time delay. Similarly to electron elastic scattering [39], it characterizes the photoelectron group delay in the dispersive potential of the ionic core. This potential includes an exchange with the core electrons [40]. In addition, the Wigner time delay in SPI is strongly affected by inter-shell correlation [41]. All these characteristics of the Wigner time delay are present in DPI. The SO adds an extra component of the time delay which is specific to DPI.

To resolve the SO process in time, one needs to use various laser-based interferometric techniques which introduce an additional component to the measurable time delay. This component, known commonly as the Coulomb laser coupling (CLC) [42] or the continuum–continuum (CC) correction [43], depends on laser frequency and the asymptotic Coulomb charge Z acting on the departing photoelectron. For the fast primary photoelectron, this

charge $Z = 1$ for the neutral targets and $Z = 0$ for the negative ions. In the former case, the fast photoelectron does not experience any CLC correction, while in the latter case, this correction is relatively small because the photoelectron is sufficiently fast. The slow electron sees the asymptotic charge $Z = 2$ for the neutral targets and $Z = 1$ for the negative ions. So while the CLC correction still affects the slow SO elecrtron, it will be relatively weaker.

References

1. Briggs, J.; Schmidt, V. Differential cross sections for photo-double- ionization of the helium atom. *J. Phys. B At. Mol. Opt. Phys.* **2000**, *33*, R1–R48. [CrossRef]
2. Avaldi, L.; Huetz, A. Photodouble ionization and the dynamics of electron pairs in the continuum. *J. Phys. B* **2005**, *38*, S861. [CrossRef]
3. Wehlitz, R. Simultaneous emission of multiple electrons from atoms and molecules using synchrotron radiation. *Adv. At. Mol. Opt. Phys.* **2010**, *58*, 1–76.
4. McGuire, J.H. *Electron Correlation Dynamics in Atomic Collisions*; Cambridge Monographs on Atomic, Molecular and Chemical Physics; Cambridge University Press: Cambridge, MA, USA , 1997.
5. Samson, J.A. Proportionality of electron-impact ionization to double photoionization. *Phys. Rev. Lett.* **1990**, *65*, 2861–2864. [CrossRef] [PubMed]
6. Kheifets, A.S. On different mechanisms of the two-electron atomic photoionization. *J. Phys. B* **2001**, *34*, L247–L252. [CrossRef]
7. Knapp, A.; Kheifets, A.; Bray, I.; Weber, T.; Landers, A.L.; Schössler, S.; Jahnke, T.; Nickles, J.; Kammer, S.; Jagutzki, O.; et al. Mechanisms of Photo Double Ionization of Helium by 530 eV Photons. *Phys. Rev. Lett.* **2002**, *89*, 033004. [CrossRef]
8. Amusia, M.Y.; Drukarev, E.G.; Gorshkov, V.G.; Kazachkov, M.P. Two-electron photoionization of helium. *J. Phys. B At. Mol. Opt. Phys.* **1975**, *8*, 1248. [CrossRef]
9. Grundmann, S.; Serov, V.V.; Trinter, F.; Fehre, K.; Strenger, N.; Pier, A.; Kircher, M.; Trabert, D.; Weller, M.; Rist, J.; et al. Revealing the two-electron cusp in the ground states of He and H_2 via quasifree double photoionization. *Phys. Rev. Res.* **2020**, *2*, 033080. [CrossRef]
10. Grundmann, S.; Trinter, F.; Bray, A.W.; Eckart, S.; Rist, J.; Kastirke, G.; Metz, D.; Klumpp, S.; Viefhaus, J.; Schmidt, L.P.H.; et al. Separating Dipole and Quadrupole Contributions to Single-Photon Double Ionization. *Phys. Rev. Lett.* **2018**, *121*, 173003. [CrossRef] [PubMed]
11. Schöffler, M.S.; Stuck, C.; Waitz, M.; Trinter, F.; Jahnke, T.; Lenz, U.; Jones, M.; Belkacem, A.; Landers, A.L.; Pindzola, M.S.; et al. Ejection of Quasi-Free-Electron Pairs from the Helium-Atom Ground State by Single-Photon Absorption. *Phys. Rev. Lett.* **2013**, *111*, 013003. [CrossRef]
12. Chang, T.N.; Poe, R.T. Double photoionization of neon. *Phys. Rev. A* **1975**, *12*, 1432–1439. [CrossRef]
13. Carter, S.L.; Kelly, H.P. Double photoionization cross section of argon. *J. Phys. B* **1976**, *9*, L565–L568. [CrossRef]
14. Carter, S.L.; Kelly, H.P. Double photoionization of neon and argon. *Phys. Rev. A* **1977**, *16*, 1525–1534. [CrossRef]
15. Pan, C.; Kelly, H.P. Photoionization cross sections of the Ar atom for production of singly and doubly charged ions near the $2p$ threshold. *Phys. Rev. A* **1989**, *39*, 6232–6240. [CrossRef]
16. Bray, I.; Fursa, D.; Kadyrov, A.; Stelbovics, A.; Kheifets, A.; Mukhamedzhanov, A. Electron- and photon-impact atomic ionisation. *Phys. Rep.* **2012**, *520*, 135–174. [CrossRef]
17. Bray, I.; Fursa, D.V.; Kheifets, A.S.; Stelbovics, A.T. Electrons and photons colliding with atoms: Development and application of the convergent close-coupling method. *J. Phys. B At. Mol. Opt. Phys.* **2002**, *35*, R117–R146. [CrossRef]
18. Pindzola, M.S.; Robicheaux, F.; Loch, S.D.; Berengut, J.C.; Topcu, T.; Colgan, J.; Foster, M.; Griffin, D.C.; Ballance, C.P.; Schultz, D.R.; et al. The time-dependent close-coupling method for atomic and molecular collision processes. *J. Phys. B* **2007**, *40*, R39–R60. [CrossRef]
19. Schultze, M.; Fiess, M.; Karpowicz, N.; Gagnon, J.; Korbman, M.; Hofstetter, M.; Neppl, S.; Cavalieri, A.L.; Komninos, Y.; Mercouris, T.; et al. Delay in Photoemission. *Science* **2010**, *328*, 1658–1662. [CrossRef]
20. Klünder, K.; Dahlström, J.M.; Gisselbrecht, M.; Fordell, T.; Swoboda, M.; Guénot, D.; Johnsson, P.; Caillat, J.; Mauritsson, J.; Maquet, A.; et al. Probing Single-Photon Ionization on the Attosecond Time Scale. *Phys. Rev. Lett.* **2011**, *106*, 143002. [CrossRef] [PubMed]
21. Mansson, E.P.; Guenot, D.; Arnold, C.L.; Kroon, D.; Kasper, S.; Dahlstrom, J.M.; Lindroth, E.; Kheifets, A.S.; L'Huillier, A.; Sorensen, S.L.; et al. Double ionization probed on the attosecond timescale. *Nat. Phys.* **2014**, *292*, 1689. [CrossRef]

22.   Kheifets, A.S.; Ivanov, I.A.; Bray, I. Timing analysis of two-electron photoemission. *J. Phys. B At. Mol. Opt. Phys.* **2011**, *44*, 101003. [CrossRef]

23.   Kheifets, A.S.; Bray, I. Time delay in two-electron photodetachment and tests of fundamental threshold laws. *Phys. Rev. Res.* **2021**, *3*, 043017. [CrossRef]

24.   Wendin, G.; Ohno, M. Strong Dynamical Effects of Many-Electron Interactions in Photoelectron Spectra from 4s and 4p Core Levels. *Phys. Scr.* **1976**, *14*, 148–161. [CrossRef]

25.   Amusia, M.Y.; Kheifets, A.S. Effect of correlations on the photoelectron spectrum of atom. *Sov. Phys.-JETP* **1984**, *59*, 710–715.

26.   Amusia, M.Y.; Kheifets, A.S. On our ability to measure the singly ionized rare-gas spectroscopic factors using the (γ,e) and (e,2e) reactions. *J. Phys. B* **1985**, *18*, L679–L684. [CrossRef]

27.   Kheifets, A.S.; Amusia, M.Y. Relativistic ab initio calculation of the xenon 5*s* ionization spectra for the (γ,e) and (e,2e) reactions. *Phys. Rev. A* **1992**, *46*, 1261–1269. [CrossRef] [PubMed]

28.   Kheifets, A.S. On the two different forms of the spectroscopic factors for the shake-up satellites. *J. Phys. B* **1994**, *27*, L463–L467. [CrossRef]

29.   Kheifets, A.S. Green's function calculation of the satellite spectrum of neon. *J. Phys. B* **1995**, *28*, 3791. [CrossRef]

30.   Kheifets, A.S.; Bray, I. Photoionization with excitation and double photoionization of helium isoelectronic sequence. *Phys. Rev. A* **1998**, *58*, 4501–4511. [CrossRef]

31.   Amusia, M.I.; Chernysheva, L.V. *Computation of Atomic Processes: A Handbook for the ATOM Programs*; Institute of Physics Publishing: Bristol, UK, 1997.

32.   Berkowitz, J. *Photoabsorption, Photoionization, and Photoelectron Spectroscopy*; Elsevier Science: Amsterdam, The Netherlands, 2012.

33.   Knapp, A.; Walter, M.; Weber, T.; Landers, A.L.; Schössler, S.; Jahnke, T.; Schöffler, M.; Nickles, J.; Kammer, S.; Jagutzki, O.; et al. Energy sharing and asymmetry parameters for photo double ionization of helium 100 eV above threshold in single-particle and Jacobi coordinates. *J. Phys. B* **2002**, *35*, L521–L526. [CrossRef]

34.   Colgan, J.; Pindzola, M.S. Double photoionization of helium at high photon energies. *J. Phys. B* **2004**, *37*, 1153–1164. [CrossRef]

35.   Kadyrov, A.S.; Bray, I. Convergent close–coupling calculations of positron–hydrogen S–wave model. *Nucl. Instr. Meth. B* **2000**, *171*, 119–125. [CrossRef]

36.   Ludlow, J.A.; Colgan, J.; Lee, T.G.; Pindzola, M.S.; Robicheaux, F. Double photoionization of helium including quadrupole radiation effects. *J. Phys. B* **2009**, *42*, 225204. [CrossRef]

37.   Kheifets, A.S.; Bray, I. Frozen core model of the double photoionization of beryllium. *Phys. Rev. A* **2002**, *65*, 012710. [CrossRef]

38.   Kheifets, A.S.; Bray, I. Valence-shell double photoionization of alkaline-earth-metal atoms. *Phys. Rev. A* **2007**, *75*, 042703. [CrossRef]

39.   Wigner, E.P. On the Behavior of Cross Sections Near Thresholds. *Phys. Rev.* **1948**, *73*, 1002–1009. [CrossRef]

40.   Rosenberg, L.; Spruch, L. Generalized Levinson theorem: Applications to electron-atom scattering. *Phys. Rev. A* **1996**, *54*, 4985–4991. [CrossRef]

41.   Kheifets, A.S. Time delay in valence-shell photoionization of noble-gas atoms. *Phys. Rev. A* **2013**, *87*, 063404. [CrossRef]

42.   Pazourek, R.; Nagele, S.; Burgdorfer, J. Time-resolved photoemission on the attosecond scale: Opportunities and challenges. *Faraday Discuss.* **2013**, *163*, 353–376. [CrossRef]

43.   Dahlström, J.; Guénot, D.; Klünder, K.; Gisselbrecht, M.; Mauritsson, J.; Huillier, A.L.; Maquet, A.; Taïeb, R. Theory of attosecond delays in laser-assisted photoionization. *Chem. Phys.* **2012**, *414*, 53–64. [CrossRef]